Coherence Control of High-order Harmonics

Salieres, P; L'Huillier, Anne; Lewenstein, M

Published in:
Physical Review Letters

DOI:
10.1103/PhysRevLett.74.3776

1995

Coherence Control of High-Order Harmonics

Pascal Salières,[1] Anne L'Huillier,[1,2] and Maciej Lewenstein[1,3,*]

[1]*Service des Photons, Atomes, et Molécules, Centre d'Etudes de Saclay, 91191 Gif-sur-Yvette, France*

[2]*Department of Physics, Lund Institute of Technology, P.O. Box 118, S-221 00 Lund, Sweden*

[3]*Institute for Theoretical Atomic and Molecular Physics, Harvard University, Cambridge, Massachusetts 02138*

(Received 15 November 1994)

We study the conditions for optimal coherence of harmonics emitted by atoms in strong laser fields. The variation of the phase of the atomic dipole moment induces a dramatic dependence of the spatial and spectral coherence on the focusing geometry. However, these coherence properties can be controlled and optimized by moving the laser focus position relative to the nonlinear medium.

PACS numbers: 32.80.Rm, 42.65.Ky

One of the most important aspects of traditional, i.e., perturbative, harmonic generation in gases or crystals is that the spatial and temporal coherence properties of the incident laser are transmitted to the generated fields. If the incident laser field is Gaussian both in space and in time, the qth harmonic pulse is also Gaussian in space and time, with a focal diameter limited by diffraction and a pulse duration determined by the Fourier transform of its spectrum. This remarkable property comes from the simple expression of the dipole moment (d_q) at the qth harmonic frequency, which, according to lowest-order perturbation theory, varies as the qth power of the incident electric field.

Recent experiments [1,2] have shown that extremely high-order harmonics can be produced in gases using intense short-pulse low-frequency lasers. These processes are highly nonperturbative. The conversion efficiency does not decrease with the process order, but remains approximately constant over a large spectral range (called "plateau"), before falling abruptly in the "cutoff" region. The dipole moment d_q is a complicated function of the laser electric field and depends, in particular, on whether the harmonic belongs to the plateau or to the cutoff. The nonlinear polarization induced in the medium is therefore a complicated function of space and time. This raises the question of the coherence of the harmonic pulses generated through these highly nonlinear processes. The recent measurements of the angular distributions [3–5] and the temporal [6] and spectral [7] profiles of high-order harmonics give only partial, if not contradictory, results. Besides its basic interest, the coherence of the harmonics is also an important issue for the use of this radiation in applications.

In this Letter, we present a theoretical study of the coherence properties of high-order harmonics generated by an intense short-pulse low-frequency laser. We show that the specific intensity dependence of the *phase* of the dipole moment in the tunneling regime [8] has a major influence on the propagation and can lead to strong spatial distortion [9] as well as spectral broadening. However, the coherence of the harmonics can be *controlled* and optimized by choosing appropriately the geometry of the interaction and, in particular, the position of the laser focus relative to the nonlinear medium. Experimental data confirm our results.

The theoretical description of harmonic generation processes involves two steps: the calculation of the single atom emission spectrum and the propagation of the generated harmonic field in the nonlinear medium. The understanding of the single atom response to an intense low-frequency laser field has progressed considerably in the last year, owing to the semiclassical ideas developed in [10,11]. The harmonics are created by those electrons which, after having tunneled through the atomic potential barrier, are accelerated by the laser field towards the nucleus and recombine. The approach developed in [8], which recovers (and justifies) this semiclassical interpretation of harmonic generation, allows us to calculate the amplitude and the phase of the dipole moment for each harmonic frequency. The second step of the theoretical description consists in solving the propagation equations in the slowly varying envelope approximation [12], using these dipole moments as source terms. In all the calculations presented in this work, we try to mimic the experimental conditions of [5]. The 825 nm wavelength laser is assumed to be Gaussian in space and time, with a 150 fs full width at half maximum (FWHM). The laser confocal parameter b is equal to 5 mm and the focus position is located at $z = 0$. The generating gas is neon and the atomic density profile is a Lorentzian function centered at z with a 0.8 mm FWHM, truncated at $z \pm 0.8$ mm. We neglect the ionization of the medium: At the highest intensity considered (6×10^{14} W/cm^2), its effect remains marginal and does not change any of the conclusions of this Letter.

The intensity dependence of the strength and phase of the 45th harmonic emitted by a single neon atom is shown in Fig. 1 [13]. In the cutoff region, $|d_{45}|^2$ increases rather steeply with the laser intensity and the phase decreases linearly, as $\sim -3.2U_p/\omega$ (ω is the laser frequency and U_p the ponderomotive energy, equal to $E^2/4\omega^2$ in atomic units, with E denoting the laser electric field). In the plateau,

 0031-9007/95/74(19)/3776(4)$06.00

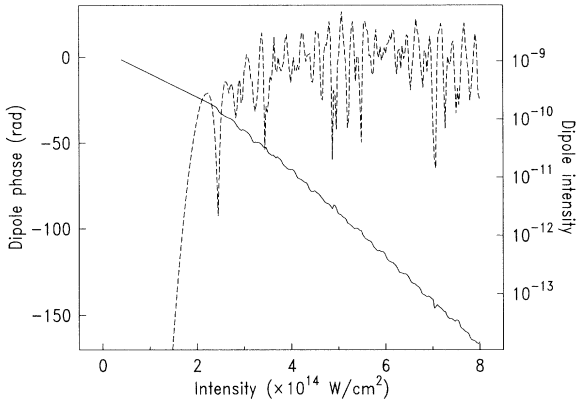

FIG. 1. 45th single neon atom harmonic intensity (dashed line) and phase (solid line) as a function of the laser intensity.

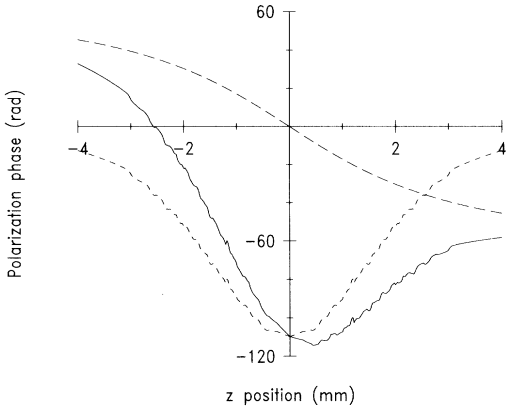

FIG. 2. Phase of the polarization on the propagation axis (solid line). The long-dashed line indicates the term due to the propagation of the fundamental, and the small-dashed line the dipole phase for a peak intensity $I_0 = 6 \times 10^{14}$ W/cm^2. The laser propagates from the left to the right.

$|d_{45}|^2$ saturates and exhibits many interferences. The phase variation is more rapid than in the cutoff region, predominantly linear ($\sim -5.8U_p/\omega$), with superimposed oscillations. These dependences, which are almost independent of the process order, can be related to the time needed for the electron to return to the nucleus. More details on this interpretation will be discussed elsewhere.

The rapid variation of the phase with intensity induces a spatially and temporally dependent phase term in the medium, which influences the generation of the macroscopic field. Harmonic generation is optimized when *phase matching* is achieved, i.e., when the difference of phase between the driving polarization and the induced field is minimized over the medium length. For the very high orders discussed here, however, the variation of the phase of the polarization is much more important than that of the induced field, so that "matching phases" amounts to minimizing the phase variation of the driving polarization. Let us consider this variation on the propagation axis at the maximum of the pulse temporal envelope. The following two terms contribute: (1) A propagation term induced by the phase shift of the Gaussian fundamental field, equal to $-q \arctan(2z/b)$, q denoting the process order. This function is shown by the long-dashed line in Fig. 2, for $q = 45$ and $b = 5$ mm. (2) The dipole phase, which depends on the z coordinate through the variation of the intensity $I(z) = I_0/(1 + 4z^2/b^2)$. It is shown by the short-dashed line in Fig. 2, for a peak intensity $I_0 = 6 \times 10^{14}$ W/cm^2. The variation of the dipole phase is less rapid outside the interval $[-3$ mm, $+3$ mm$]$, when the intensity on axis corresponds to the cutoff region [$I(z) \leq 2.4 \times 10^{14}$ W/cm^2; see Fig. 1]. The total phase of the nonlinear polarization is represented by the solid line. In the region $z < 0$, the variations of both phases add, leading to a rapid decrease of the total phase. In the region $z > 0$, they have opposite signs, and almost compensate when the intensity on axis corresponds to the cutoff region. Consequently, phase matching strongly depends on the position of the medium relative to the laser focus. The best phase matching conditions *on axis* are those for which the phase variation of the polarization over the medium length ($\sim$1 mm) is minimal, i.e., when the laser is focused approximately 3 mm *before* the generating medium.

In Fig. 3, we study the variation of the conversion efficiency for the 45th harmonic generation as a function of the position (z) of the center of the atomic medium (relative to the laser focus placed in $z = 0$), for a peak

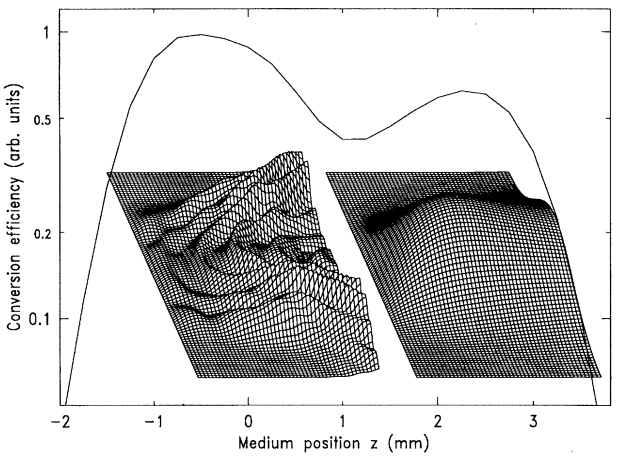

FIG. 3. Conversion efficiency for the 45th harmonic (arb. units) as a function of the position of the center of the medium z, at a peak intensity of 6×10^{14} W/cm^2. The 3D plots show how the harmonic field is constructed in the medium at $z = -1$ (left) and $z = 3$ (right). The field $|E_q(R, Z)|$ (vertical axis) is plotted as a function of Z (horizontal axis) and R (direction perpendicular to the plane of the figure).

intensity, i.e., at best focus and at the maximum of the pulse envelope, of 6×10^{14} W/cm^2. The result, shown as a solid line, is quite asymmetric, and exhibits two maxima. To understand their origin, we present three-dimensional (3D) plots showing how the field is generated in the nonlinear medium at $z = -1$ mm (left) and $+3$ mm (right). The maximum on the positive side (when the laser is focused before the medium) corresponds to the best phase matching conditions on axis (see Fig. 2). The field is constructed in a regular way, along the propagation axis (see the 3D plot on the right). This occurs when the intensity *in the medium* is such that the harmonic is close to the cutoff. The maximum on the negative side, closer to the laser focus, corresponds to a rather distorted interference pattern in the medium. The intensity is such that the harmonic is in the plateau region with rapid phase and amplitude variations, in both the longitudinal and transverse directions. Moreover, on this side of the focus, efficient harmonic generation on axis is prevented by the rapid variation of the polarization phase (see Fig. 2). However, as shown by the 3D plot on the left side in Fig. 3, the phase variation can be minimized along favored directions *off* the propagation axis. This leads to the formation of relatively intense annular beams.

In Fig. 4, we examine the coherence properties of the 45th harmonic for the same positions z of the gas medium as the 3D plots: 3 and -1 mm. They correspond to comparable efficiencies (see Fig. 3), even though the respective intensities in the medium are different. For a peak intensity $I_0 = 6 \times 10^4$ W/cm^2, $I(z = 3) = 2.5 \times 10^{14}$ W/cm^2 (close to the cutoff region), and $I(z = -1) = 5.2 \times 10^{14}$ W/cm^2 (plateau). Figure 4(a) presents the spatial profiles at the exit of the medium (i.e., $z + 0.8$ mm). When the laser is focused 3 mm before the medium, the harmonic profile (solid line) is very regular with a super-Gaussian shape of half-width at $1/e^2$ equal to 18 μm (compared to 45 μm for the fundamental). This is the result of efficient phase matching on axis together with a regular intensity dependence of the dipole amplitude in the cutoff region. The harmonic radial phase at the maximum of the pulse temporal envelope presents a regular parabolic behavior, and corresponds to a spherical phase front diverging from a virtual source coinciding with the focus of the fundamental beam. The harmonic beam is thus broader and more divergent than predicted by perturbation theory. Its far-field profile, calculated through a Hankel transform, exhibits similar shape and divergence [Fig. 4(b)]. These results are in good agreement with previous experimental data for the 45th harmonic presented in [5].

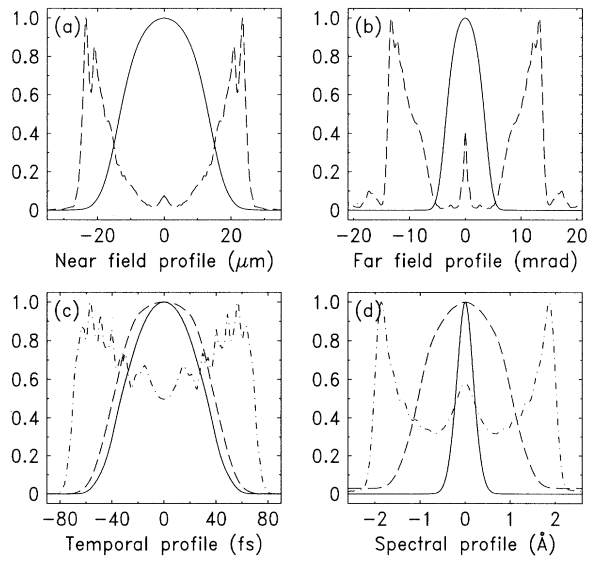

FIG. 4. (a) Near-field, (b) far-field, (c) temporal, and (d) spectral profiles of the 45th harmonic. The solid line is the result obtained at $z = 3$ mm, and the dashed line the result at $z = -1$ mm. The dot-dashed line in both (c) and (d) indicates the result obtained at $z = 0$.

In contrast, when the laser is focused 1 mm after the medium, the spatial profile becomes annular, with an external radius of about 25 μm (as large as the fundamental one) and very little energy emitted on axis [dashed line in Fig. 4(a)]. This is the consequence of phase matching off axis (see Fig. 3), resulting in the formation of annular beams. Moreover, the phase at the maximum of the temporal envelope varies rapidly in the transverse direction, which leads to a distorted annular beam in the far field with a divergence even larger than the 10 mrad half-width at $1/e^2$ of the Gaussian laser beam. Both beams are almost spatially separated in the far field, the harmonic beam being outside the fundamental.

The variation of the dipole phase with intensity has also significant effects regarding the temporal coherence properties of the harmonic radiation. Figure 4(c) shows the temporal profiles of the 45th harmonic obtained at $z = +3$ (solid line) and -1 mm (dashed line). They are very regular, with 70 and 80 fs FWHM, respectively. For these positions, phase matching is efficient only for intensities close to the maximum of the laser temporal envelope. Consequently, the harmonic pulses are narrow and regular. In contrast, for intermediate z positions, phase matching can be more efficient at lower intensities, leading to distorted temporal profiles sometimes as large as the fundamental. As an example, we show as a dot-dashed line the result obtained when the center of the medium coincides with the laser focus ($z = 0$).

In addition, the dipole phase intensity dependence induces a *phase modulation* of the harmonic pulse. This leads to spectral broadening which, as the spatial profiles, strongly depends on the position of the medium relative to the laser focus. Figure 4(d) presents the spectral profiles of the 45th harmonic for the same z positions as before. When $z = 3$ mm (solid line), the harmonic is mainly created in the cutoff region where the intensity dependence of the dipole phase is slow, so that the

frequency chirp is limited. The FWHM is 0.4 Å, which corresponds to about 4 times the Fourier transform limit. In contrast, when $z = -1$ mm (dashed line), the intensity in the medium corresponds to the plateau region; the dipole phase varies much more rapidly with intensity, leading to a significant broadening. The width of the corresponding spectrum is more than 4 times that of the previous one. For comparison, we also show the result obtained at $z = 0$ (dot-dashed line), which presents a very distorted spectrum with a 4 Å width. The asymmetry observed in the conversion efficiency and in the spatial properties of the harmonics relative to $z = 0$ exists also for the temporal coherence properties. Both temporal and spectral profiles are quite different, for example, at $z = 1$ and -1 mm, though the laser intensity in the medium is the same. This is because phase matching occurs in a different way, due to the asymmetry introduced by the variation of the dipole phase. Both spatial and temporal coherence of the harmonics are thus quite intertwined, in contrast to traditional, perturbative, harmonic generation.

Finally, we present experimental evidence for the importance of the geometrical conditions for the coherence of the generated harmonics. In Fig. 5(a), we show the evolution with z of the far-field profile of the 39th harmonic at an intensity of 3×10^{14} W/cm^2. We choose this particular harmonic and intensity for comparing with experimental results presented in Fig. 5(b). These experimental results have been obtained in neon, with a 825 nm 150 fs Cr:LiSAF laser, at relatively low laser intensity, below the saturation intensity for ionization. They will be presented in more detail elsewhere. The evolution from Gaussian beams to increasingly distorted annular profiles is remarkably reproduced in our calculations.

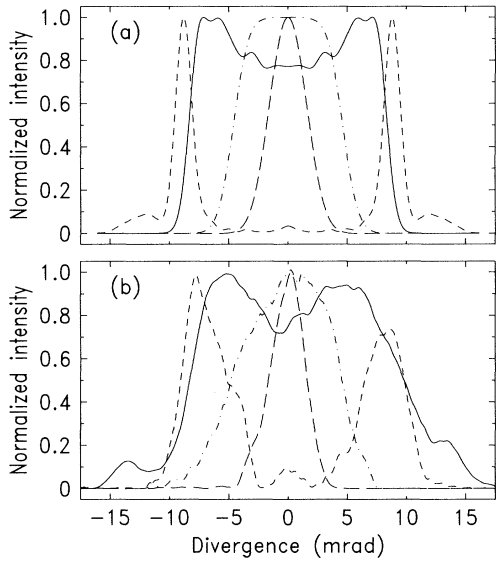

FIG. 5. Theoretical (a) and experimental (b) evolution of the 39th harmonic far-field profile as a function of the position of the medium relative to the focus. As z decreases, the profile, first quite narrow (long-dashed line), broadens (dot-dashed line), presents a dip at the center (solid line), and, finally, when z is negative, becomes a ring (small-dashed line).

In conclusion, the intensity dependence of the phase of the dipole affects dramatically the spatial and the spectral coherence of the emitted beam. However, by focusing the laser sufficiently before the medium, it is possible to generate high-order harmonics with good spatial and temporal coherence properties, while keeping a reasonable conversion efficiency.

The experimental results [Fig. 5(b)] have been obtained in collaboration with T. Ditmire and M. D. Perry at the Lawrence Livermore National Laboratory. We are grateful to Ph. Balcou for a critical reading of the manuscript. M.L. was supported by the Centre d'Etudes de Saclay and by the NSF Grant for the Institute for Theoretical Atomic and Molecular Physics at Harvard-Smithonian Observatory.

*Permanent address: Centrum Fizyki Teoretycznej PAN, Al. Lotników 32/46, 02–668 Warsaw, Poland.

[1] J. J. Macklin, J. D. Kmetec, and C. L. Gordon III, Phys. Rev. Lett. **70**, 766 (1993).

[2] A. L'Huillier and Ph. Balcou, Phys. Rev. Lett. **70**, 774 (1993).

[3] J. Peatross and D. D. Meyerhofer, Phys. Rev. A **51**, R906 (1995).

[4] J. W. G. Tisch, R. A. Smith, J. E. Muffet, M. Ciarrocca, J. P. Marangos, and M. H. R. Hutchinson, Phys. Rev. A **49**, R28 (1994).

[5] P. Salières, T. Ditmire, K. S. Budil, M. D. Perry, and A. L'Huillier, J. Phys. B **27**, L217 (1994).

[6] M. E. Faldon, M. H. R. Hutchinson, J. P. Marangos, J. E. Muffet, R. A. Smith, J. W. G. Tisch, and C.-G. Wahlström, J. Opt. Soc. Am. B **9**, 2094 (1992).

[7] C.-G. Wahlström, J. Larsson, A. Persson, T. Starczewski, S. Svanberg, P. Salières, Ph. Balcou, and A. L'Huillier, Phys. Rev. A **48**, 4709 (1993).

[8] M. Lewenstein, Ph. Balcou, M. Yu. Ivanov, A. L'Huillier, and P. Corkum, Phys. Rev. A **49**, 2117 (1994).

[9] The influence of intensity-dependent phases on the angular distributions has been pointed out in J. Peatross, M. V. Fedorov, and K. C. Kulander, J. Opt. Soc. Am. B (to be published), and in J. E. Muffet, C.-G. Wahlström, and M. H. R. Hutchinson, J. Phys. B **27**, 5693 (1994).

[10] J. L. Krause, K. J. Schafer, and K. C. Kulander, Phys. Rev. Lett. **68**, 3535 (1992); K. C. Kulander, K. J. Schafer, and J. L. Krause, in *Super-Intense Laser-Atom Physics,* edited by B. Piraux, A. L'Huillier, and K. Rzążewski, NATO ASI, Ser. B, Vol. 316 (Plenum Press, New York, 1993), p. 95.

[11] P. B. Corkum, Phys. Rev. Lett. **71**, 1994 (1993).

[12] A. L'Huillier, Ph. Balcou, S. Candel, K. J. Schafer, and K. C. Kulander, Phys. Rev. A **46**, 2778 (1992).

[13] This phase dependence has been also noted in [1], using a related model of W. Becker, S. Long, and J. K. McIver, Phys. Rev. A **50**, 1540 (1994).